The current issue and full text archive of this journal is available at
www.emeraldinsight.com/0264-4401.htm

Structural dynamic analysis using Gaussian process emulators

F.A. DiazDelaO and S. Adhikari
School of Engineering, Swansea University, Swansea, UK

Received 26 March 2009
Revised 2 September 2009
Accepted 4 September 2009

Abstract

Purpose – In the dynamical analysis of engineering systems, running a detailed high-resolution finite element model can be expensive even for obtaining the dynamic response at few frequency points. To address this problem, this paper aims to investigate the possibility of representing the output of an expensive computer code as a Gaussian stochastic process.

Design/methodology/approach – The Gaussian process emulator method is discussed and then applied to both simulated and experimentally measured data from the frequency response of a cantilever plate excited by a harmonic force. The dynamic response over a frequency range is approximated using only a small number of response values, obtained both by running a finite element model at carefully selected frequency points and from experimental measurements. The results are then validated applying some adequacy diagnostics.

Findings – It is shown that the Gaussian process emulator method can be an effective predictive tool for medium and high-frequency vibration problems, whenever the data are expensive to obtain, either from a computer-intensive code or a resource-consuming experiment.

Originality/value – Although Gaussian process emulators have been used in other disciplines, there is no knowledge of it having been implemented for structural dynamic analyses and it has good potential for this area of engineering.

Keywords Gaussian processes, Bayesian statistical decision theory, Stochastic processes, Structural analysis, Programming and algorithm theory

Paper type Research paper

1. Introduction

Many engineering dynamical systems are complex enough to render physical experimentation impossible. As a consequence, these systems are often investigated running computer codes involving the finite element method (Zienkiewicz and Taylor, 1991; Bathe, 1995; Cook *et al.*, 2001; Hughes, 2000; Petyt, 1998). Dynamic analyses of large engineering systems such as aircrafts, helicopters, and space shuttles usually employ a finite element model with well over several million degrees of freedom. O'Hagan (2006) refers to such finite element analysis codes, as well as to the underlying mathematical models, as simulators. In mathematical terms, a simulator is a function $\eta\colon\ \mathbb{R}^{d_1} \rightarrow \mathbb{R}^{d_2}$ that given an input $\mathbf{x}$, it produces an output $\mathbf{y} = \eta(\mathbf{x})$. Simulators are a common tool when studying intricate phenomena in a wide range of disciplines. However, they can have a high cost of execution, measured in terms of employed CPU time, number of floating point operations performed, or required computer capability. Consider the example given by Goldstein (2007), in which sophisticated climate models

The first author gratefully acknowledges the support of the Engineering and Physical Sciences Research Council (EPSRC) for the award of a studentship through an ideas Factory grant and Consejo Nacional de Ciencia y Tecnología (CONACYT) for the award of a scholarship from the Mexican Government. The second author gratefully acknowledges the support of EPSRC through the award of an Advanced Research Fellowship and The Leverhulme Trust for the award of the Philip Leverhulme Prize.

Engineering Computations: International Journal for Computer-Aided Engineering and Software
Vol. 27 No. 5, 2010
pp. 580-605

0264-4401
DOI 10.1108/02644401011050895

can take months to complete a single run. Similarly, Thomke *et al.* (1999) noted the prodigious computer power needed to simulate the outcome of a rollover car accident. The terms "expensive" and "computer intensive" are used indistinctly throughout this paper. The same applies to "simulator" and "model". Additionally, the input $\mathbf{x}$ for the simulators studied here is interpreted as a frequency level ω.

Several strategies have been devised to reduce the computational cost of expensive simulators. Based on different underlying methodologies, these strategies are referred to as metamodels, response surfaces, surrogates, auxiliary models, among others (Kleijnen 2009). They have been extensively applied in engineering. For example, Craig *et al.* (2005) performed variable screening and optimization in crashworthiness design based on a response surface methodology. Fan *et al.* (2006) incorporate surrogate modelling to multi-objective optimization. Pérez *et al.* (2008) solved nonlinear optimization problems using quadratic response surfaces. Sultan (2007) applied surrogate modelling to replace an expensive iterative procedure used to prevent rotor-housing interference in a fluid processing machine. Metamodel-based design optimization has also been applied by Zhao *et al.* (2008).

Yet another type of metamodelling approach, which has been in constant development over the last two decades, is Gaussian process emulation. Based on the analysis and design of computer experiments pioneered by Satner *et al.* (2003) and Sacks *et al.* (1989), and using concepts of Bayesian statistics, such technology consists in constructing an approximation to the simulator, called an emulator. More precisely, an emulator is a statistical approximation to the simulator. Not only does it approximate $\eta(\cdot)$, it provides a probability distribution for it. Broadly speaking, emulation works in the following way: A small and carefully selected set of code runs is treated as training data used to update the prior beliefs about the simulator. As it will be seen later, these beliefs are expressed as a Gaussian stochastic process prior distribution. After conditioning on the training runs and updating the prior distribution, the mean of the resulting posterior distribution approximates the output of the simulator at any untried input, whereas it reproduces the known output of the simulator at each initial input.

Gaussian process emulators have already been implemented in a number of different scientific fields. Kennedy *et al.* (2006) presented three case studies related to environmental computer models. They emulated a vegetation dynamic model, a model of ecosystem photosynthesis and water balance, and finally a model that estimates the UK's carbon budget. Challenor *et al.* (2006) emulated what they consider to be a moderately complex climate model. Rougier (2007) presented another application to a climate model. Bates *et al.* (2006) emulated a model of a complete revolution of a piston's shaft. Haylock and O'Hagan (1996) emulated a model of doses to organs of the body after ingestion of a radioactive substance. Oakley and O'Hagan (2004) worked with a simulator of the cost resulting from bone fractures for patients suffering from osteoporosis. Authors such as McFarland *et al.* (2008) noted that Gaussian process emulation is in most cases equivalent to the family of methods called kriging predictors. Using this terminology, Simpson *et al.* (2001) examined the difficulties in creating global approximations in the context of multidisciplinary design optimization. Bearing in mind all this previous research and considering that complex structural dynamic models are prone to the use of computer intensive simulators, it is natural to think about the potential benefit from the application of emulators in structural dynamics.

The paper is organized as follows: in section 2, the structural dynamic model to be emulated is introduced. In section 3, the mathematical theory behind emulators is

briefly reviewed. A simulator of the frequency response function (FRF) of a simple damped spring-mass system with three degrees of freedom is used as an introductory example. In section 4, the capabilities of emulators are tested, applying them to systems with thousands of degrees of freedom. The frequency response of several systems with a number of degrees of freedom ranging from 1,200 to 4,650 is emulated. In section 5, the applicability of emulators in a circumstance in which there is no mathematical/computational model available for a given phenomenon, due perhaps to the lack of knowledge of the physics of the system, is explored. The results are compared with data taken from an experiment performed by Adhikari *et al.* (2009). In section 6, the obtained results are discussed. Finally, section 7 presents some measures to assess the adequacy of Gaussian process emulators as valid representations of simulators.

2. Damped structural dynamics

In this section, the problem of modelling the response of a damped structural system subject to different frequency ranges of vibration is considered. Viscous damping is the most common model for representing vibration damping in linear systems. First introduced by Rayleigh (1877), this model assumes that the instantaneous generalized velocities are the only relevant variables that determine damping. Viscous damping models are used widely for their simplicity and mathematical convenience even though the behavior of real structural materials is, at best, poorly mimicked by simple viscous models. For this reason it is well recognized that in general a physically realistic model of damping will not be viscous. Damping models in which the dissipative forces depend on any quantity other than the instantaneous generalized velocities are nonviscous damping models. Mathematically, any causal model which makes the energy dissipation functional nonnegative is a possible candidate for a nonviscous damping model. Clearly a wide range of choice is possible, either based on the physics of the problem, or by a priori selecting a model and fitting its parameters from experiments. For the sake of generality, this paper considers nonviscously (or viscoelastically) damped systems (Torvik and Bagley, 1987; Woodhouse, 1998; Maia *et al.*, 1998; Adhikari, 2002; Adhikari and Woodhouse, 2003). The equations of motion of a N-degree-of-freedom linear system with such damping can be expressed by:

$$\mathbf{M}\ddot{\mathbf{q}}(t) + \int_0^t \mathcal{G}(t-\tau)\dot{\mathbf{q}}(\tau)d\tau + \mathbf{K}\mathbf{q}(t) = \mathbf{f}(t) \tag{1}$$

where $\mathbf{q}(t) \in \mathbb{R}^N$ is the displacement vector, $\mathbf{f}(t) \in \mathbb{R}^N$ is the forcing vector, $\mathbf{M} \in \mathbb{R}^{N\times N}$ is the mass matrix, $\mathbf{K} \in \mathbb{R}^{N\times N}$ is the stiffness matrix and $\boldsymbol{\mathcal{G}}(t) \in \mathbb{R}^{N\times N}$ is the matrix of damping kernel functions. The kernel functions $\boldsymbol{\mathcal{G}}(t)$ are known as retardation functions, heredity functions, after-effect functions or relaxation functions in the context of different subjects. Early works in this area can be traced back to Biot (1958) in the context of viscoelastic materials. In the limit when $\boldsymbol{\mathcal{G}}(t-\tau) = \mathbf{C}\delta(t-\tau)$, where $\delta(t)$ is the Dirac-delta function, equation (1) reduces to the case of viscous damping. Taking the Fourier transform of equation (1), the equation of motion in the frequency domain can be expressed in terms of the excitation frequency level, $\omega \in [0, \ldots, \infty)$ as:

$$\mathbf{D}(\omega)\overline{\mathbf{q}}(\omega) = \overline{\mathbf{f}}(\omega) \tag{2}$$

where $\overline{\mathbf{q}}(\omega)$ and $\overline{\mathbf{f}}(\omega)$ are the Fourier transforms of $\mathbf{q}(t)$ and $\mathbf{f}(t)$, respectively. The

dynamic stiffness matrix $\mathbf{D}(\omega)$ is the complex symmetric matrix given by:

$$\mathbf{D}(\omega) = -\omega^2\mathbf{M} + i\omega\mathbf{G}(\omega) + \mathbf{K} \tag{3}$$

where $\mathbf{G}(\omega)$ is the Fourier transform of $\boldsymbol{\mathcal{G}}(t)$. Provided that $\mathbf{D}(\omega)^{-1}$ exists, the response vector becomes $\overline{\mathbf{q}}(\omega) = \mathbf{D}(\omega)^{-1}\overline{\mathbf{f}}(\omega)$. Suppose there is interest in working with some linear function of the elements of $\overline{\mathbf{q}}(\omega)$, namely:

$$\phi(\omega) = \mathbf{Q}\overline{\mathbf{q}}(\omega) = \mathbf{Q}\mathbf{D}(\omega)^{-1}\overline{\mathbf{f}}(\omega) \tag{4}$$

where $\mathbf{Q}$ is a rectangular matrix. Since $\phi(\cdot)$ is a complex-valued function, only its modulus is relevant in practice. That way, let:

$$\eta(\omega) = \left|\mathbf{Q}\mathbf{D}(\omega)^{-1}\overline{\mathbf{f}}(\omega)\right| \tag{5}$$

For systems with general nonproportional damping as considered here, it is in general not possible to represent the response in terms of undamped modes. In such cases the response needs to be expressed in terms of the complex modes of the system (Adhikari, 1999, 2004). The computation of complex modes is numerically much more expensive as the size of the eigenvalue problem doubles (Newland, 1989) due to the use of the state-space approach. For systems with general frequency-dependent viscoelastic damping models, a higher-order nonlinear complex eigenvalue problem (Adhikari, 2001b; Wagner and Adhikari, 2003; Adhikari and Wagner, 2003) needs to be solved in order to obtain the dynamic response in terms of the modal series. The solution of such eigenvalue problems is significantly more expensive compared to even nonproportional viscously damped systems. Adhikari and Wagner (2004) showed that for such system a direct integration scheme in the time-domain can be more efficient compared to the modal approach. In this paper, the alternative approach of obtaining the response by solving the linear system (2) for only few frequency points is explored. In such context, a Gaussian process emulator might be a convenient choice. In the following section the basic theory on the implementation of emulators is briefly discussed.

3. Gaussian process emulators

3.1 Introductory example

Suppose that n design points, namely $\omega_1, \ldots, \omega_n$, are chosen in the input domain of the simulator $\eta(\cdot)$. The set $\{\eta(\omega_1), \ldots, \eta(\omega_n)\}$, resulting from the evaluation of $\eta(\cdot)$ in each of the design points, is called training set. Following O'Hagan (2006), an emulator should satisfy some minimal criteria:

- Since by definition the output at each design point is known, the emulator should reproduce this output with no uncertainty.
- At any ω that is not a design point, the probability distribution provided by the emulator should produce a mean value that constitutes a plausible interpolation/extrapolation of the training data. The probability distribution around this predictive mean should also express the uncertainty about how the emulator might interpolate/extrapolate.

In addition to these criteria, Rougier *et al.* (2007) note that the key feature of an emulator is that it quantifies the uncertainty that arises from having a training set with

limited size. Naturally, it is also desirable that emulation is at least as efficient as other available techniques, if it is to be worthy of implementation.

To have a better understanding of what do the above criteria mean, consider the simple three-degree-of-freedom spring-mass system shown in Figure 1. For purposes of illustration, the simulator of the corresponding FRF is regarded as if it were computer intensive.

Let the mass of each block be 1 kg, the stiffness of each spring be 1 N/m, and the viscous damping constant of the damper associated with each block be 0.8 Ns/m. The mass, stiffness, and damping matrices of this simple system can be obtained as:

$$\mathbf{M} = \begin{bmatrix} m & 0 & 0 \\ 0 & m & 0 \\ 0 & 0 & m \end{bmatrix}, \quad \mathbf{K} = \begin{bmatrix} 2k & -k & 0 \\ -k & 2k & -k \\ 0 & -k & 2 \end{bmatrix}$$

and

$$\mathbf{G}(\omega) = \frac{\lambda}{\lambda + i\omega} \begin{bmatrix} c & 0 & 0 \\ 0 & 0 & 0 \\ 0 & 0 & c \end{bmatrix} \tag{6}$$

where $m = 1$, $k = 1$, $c = 0.8$, and λ, the relaxation parameter, is chosen to be equal to the first natural frequency of the system. Note that the system has nonproportional damping. Let the forcing vector be $\mathbf{f} = [0, 1, 0]^T$. In that case, the FRF corresponding to the ℓ th degree of freedom has the following form:

$$\phi_\ell(\omega) = \mathbf{D}(\omega)_\ell^{-1} \bar{\mathbf{f}}(\omega) \tag{7}$$

where $\mathbf{D}(\omega)_\ell^{-1}$ denotes the ℓth row of $\mathbf{D}(\omega)^{-1}$, for $\ell = 1, \ldots, 3$. Since $\phi_\ell(\cdot)$ is a complex-valued function, the simulator for ℓ fixed is the following single-variable function:

$$\eta(\omega) = |\phi_\ell(\omega)| = \left| \mathbf{D}(\omega)_\ell^{-1} \bar{\mathbf{f}}(\omega) \right| \tag{8}$$

Figure 2(a) shows the case when $\ell = 3$ and 13 training runs (the circles) are used. The predictive mean of the emulator (the dots) approximates the values of the simulator (the solid line) at several untried inputs throughout the input domain. On the other hand, it reproduces the output of the simulator at each of the training points. Note how the approximation improves when more training runs are used, as shown in Figure 2(b).

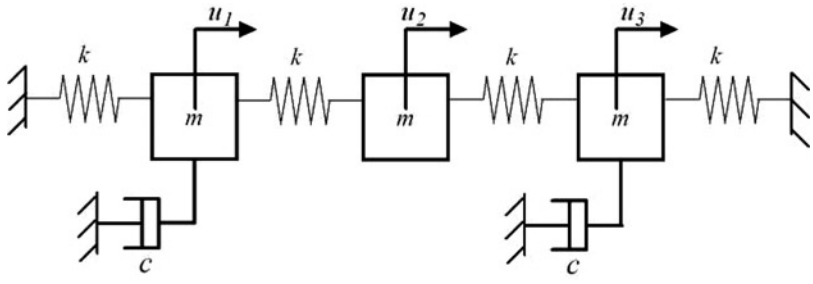

Notes: m = 1 kg, k = 1 N/m, c = 0.8 Ns/m

Figure 1.
Three-degree-of-freedom damped spring-mass system

Additionally, Figure 3 shows upper and lower bounds of two standard deviations for the predictive mean. As the number of training runs increases, there is a reduction of the uncertainty in the value of the predictive mean. Note how the uncertainty is equal to zero in each of the training runs, as it would be expected, since the emulator reproduces the simulator's output at these points. Observe however that for both cases, the uncertainty increases rapidly when extrapolating the training set.

3.2 Theoretical background

Let $\eta(\cdot)$ be an expensive simulator, such that it is practical to evaluate it only at a limited number of inputs. This allows $\eta(\cdot)$ to be regarded as a random variable in the sense that the output is unknown until the simulator is actually run. A Bayesian treatment is followed here, whereby prior beliefs about the relationship between the input and the unknown output are conditioned on a set of evaluations of $\eta(\cdot)$, thus combining subjective and objective information. Begin by assuming that $\eta(\cdot)$ admits the following stochastic representation:

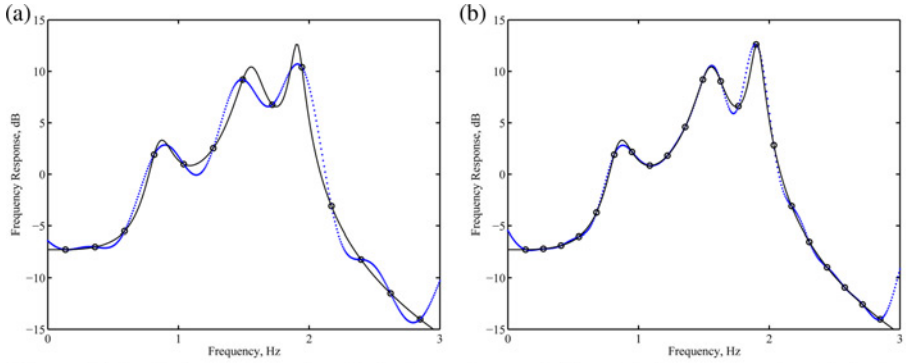

Notes: (a) Predictive mean using 13 design points and (b) predictive mean using 21 design points; the forcing vector is $[0, 1, 0]^T$; (-): simulator's output, (o): training runs, (···): emulator's predictive mean

Figure 2.
Emulation of $\eta(\omega) = |\phi_3(\omega)|$ for a damped spring-mass system with 3 degrees of freedom

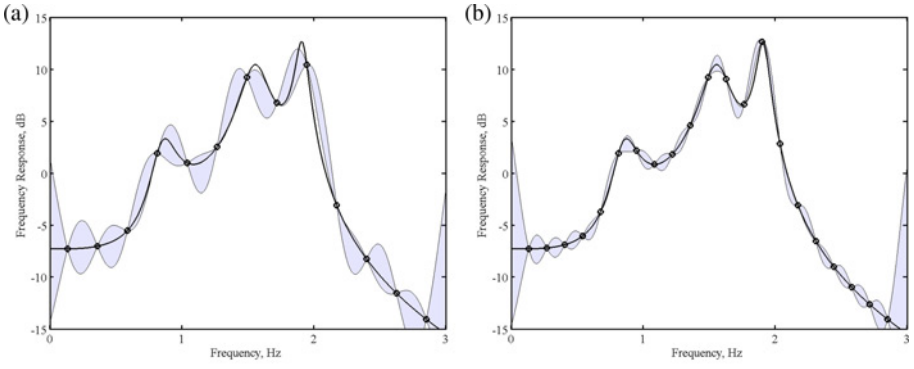

Notes: (a) Uncertainty using 13 design points and (b) uncertainty using 21 design points; the forcing vector is $[0, 1, 0]^T$; (-): simulator's output, (o): training runs; the shaded areas are probability bounds for the predictive mean

Figure 3.
Emulation of $\eta(\omega) = |\phi_3(\omega)|$ for a damped spring-mass system with 3 degrees of freedom

$$\eta(\omega) = \mathbf{h}(\omega)^T \boldsymbol{\beta} + Z(\omega) \tag{9}$$

where $\mathbf{h}(\cdot)$ is a vector of known functions of ω and β is a vector of unknown coefficients. The function $Z(\cdot)$ is assumed to be a stochastic process with mean zero and some covariance function of ω. An advantageous choice for $Z(\cdot)$ is the Gaussian stochastic process.

Definition. Gaussian stochastic process: Let $\mathcal{X} \subseteq \mathbb{R}^d$. Then $Z(\mathbf{x})$ for $\mathbf{x} \in \mathcal{X}$ is a Gaussian stochastic process if for any $L \geq 1$ and any choice $\{\mathbf{x}_1, \ldots, \mathbf{x}_L\} \subseteq \mathcal{X}$, the vector $[Z(\mathbf{x}_1), \ldots, Z(\mathbf{x}_L)]^T$ has a multivariate normal distribution.

As noted by Kennedy and O'Hagan (2001), the choice of a Gaussian process is made for much the same reasons that the Gaussian distribution repeatedly appears in statistics: it is analytically tractable, flexible, and quite often realistic. Despite these advantages, they are careful to refer to alternative ways of expressing prior beliefs available in the literature. One such approach is to represent $\eta(\cdot)$ as a linear combination of basis functions such as splines, wavelets, and sigmoidal functions. Suppose a linear structure of the form $\mathbf{h}(\cdot)^T \boldsymbol{\beta}$, where $\mathbf{h}(\cdot)$ is a vector of regression functions and β is a vector of coefficients, is chosen to model the prior mean of $\eta(\cdot)$. Then, the interpretation of equation (9) becomes clearer. That is, $\eta(\cdot)$ is assumed to deviate from the mean of its distribution following a Gaussian stochastic process. Oakley and O'Hagan (2004) note that the choice of $\mathbf{h}(\cdot)$ is arbitrary, although it should be chosen to reflect the available information about the functional form of $\eta(\cdot)$. In the particular case of structural dynamics, the mathematical structure of an FRF is well known and could be taken into account when selecting $\eta(\cdot)$. This is currently an area for further investigation.

An important assumption is to regard $\eta(\cdot)$ as a continuous function of its inputs. It follows that if ω and ω' are close together, then the values of $\eta(\omega)$ and $\eta(\omega')$ should also be close. It is therefore reasonable to think that the correlation between $\eta(\omega)$ and $\eta(\omega')$ increases when the distance between ω and ω' decreases and viceversa. This implies that each element of the training set provides considerable information about $\eta(\cdot)$ for inputs close to the corresponding design points. Hence, the uncertainty about the value of untried inputs is reduced as the number of design points increases because the maximum distance from any design point decreases (recall criterion 2 above).

The discussion on how to determine suitable covariance functions can become very technical and further details can be consulted in Satner *et al.* (2003). A popular choice for covariance function is the one that is adopted hereafter, namely:

$$Cov(\eta(\omega), \eta(\omega')) = \sigma^2 C(\cdot, \cdot) \tag{10}$$

with the correlation function $C(\cdot,\cdot)$ such that:

$$C(\cdot, \cdot) = e^{-(\omega-\omega')^T \mathbf{B}(\omega-\omega')} \tag{11}$$

where $\mathbf{B}$ is a positive-definite diagonal matrix. Observe that $C(\omega, \omega) = 1$ and that it decreases as the distance between two points increases, as required.

As a consequence of the above, the prior knowledge about $\eta(\cdot)$, given β and σ^2, is represented as having a Gaussian process distribution with mean $\mathbf{h}(\cdot)^T \beta$ and covariance expressed by equation (10). The latter is symbolized by:

$$\eta(\cdot)|\beta, \sigma^2 \sim \mathcal{N}(\mathbf{h}(\cdot)^T\beta, \sigma^2 C(\cdot,\cdot)) \tag{12}$$

The subjective information about the input and the unknown outputs is contained in this prior distribution. The next step is to update it by adding the objective information contained in a vector of observations, denoted here by $\mathbf{y} = [\eta(\omega_1), \ldots, \eta(\omega_n)]^T$. It can be shown that this updating yields a posterior distribution of the form:

$$\eta(\cdot)|\mathbf{y}, \sigma^2 \sim \mathcal{N}(m^{**}(\cdot), \sigma^2 C^{**}(\cdot,\cdot)) \tag{13}$$

where the posterior mean $m^{**}(\cdot)$ does not depend on $\eta(\cdot)$. It thus provides a fast approximation of $\eta(\omega)$ for any ω (recall again criterion 2 above). For the explicit expressions of $m^{**}(\cdot)$ and $C^{**}(\cdot,\cdot)$, as well as an outline of the analysis that results in the posterior distribution (13), refer to the Appendix.

In light of the above discussion, the algorithm to approximate the simulator defined by equation (5) is the following.

Emulation algorithm.

- Select an initial design of frequency values $\omega_1, \ldots, \omega_n$.
- Obtain the vector of observations $\mathbf{y} = [\eta(\omega_1), \ldots, \eta(\omega_n)]^T$.
- Update the prior distribution (12), which contains subjective information, by adding the objective information **y**. This enables the calculation of $m^{**}(\cdot)$, the predictive mean of the posterior distribution (13) given the data **y**. As already mentioned, such mean provides an approximation of $\eta(\omega)$ for any ω.

In the above algorithm, the selection of an initial design in step (1) must be done carefully. It would be ideal to extract the most information about $\eta(\cdot)$ out of the minimum number of evaluations possible. The choice of the initial design is an active research area. A copious amount of literature on the subject is available. An account of existing strategies can be consulted in Satner *et al.* (2003). Throughout this paper, the Latin hypercube sampling strategy proposed by Mckay *et al.* (1979) is employed. Latin hypercube sampling can be viewed as an extension of Latin square designs to higher dimensions, where each dimension is guaranteed to be fully represented.

It was previously assumed that $\eta(\cdot)$ is a continuous function of its inputs. Additionally, the correlation function between any two inputs, ω and ω', was defined by equation (11). A crucial component of such correlation function is the diagonal matrix **B**, which contains what are known as smoothness parameters. Intuitively, these parameters specify how far an untried input needs to go from a design point before the uncertainty becomes appreciable. In other words, they quantify the rate at which the output varies as the one input changes. The technique to estimate the smoothness parameters used in this paper is to derive the density function $f(\mathbf{B}|\mathbf{y})$ and obtain a maximum likelihood estimator. The details can be found in Haylock (1996).

4. Numerical example: frequency response of a cantilever plate

Consider a finite element model of a rectangular steel plate 998 mm long, 530 mm wide, 3 mm thick, and with a mass of 12.47 kg. Suppose it is clamped along a short edge and that it has a damping patch attached to it, as shown in Figure 4. The resulting damping is nonproportional, since the corresponding damping matrix becomes a block matrix with some zeros along the diagonal. Hence, it cannot be represented as a positive linear combination of the mass and stiffness matrices whose diagonals are nonzero (Caughey

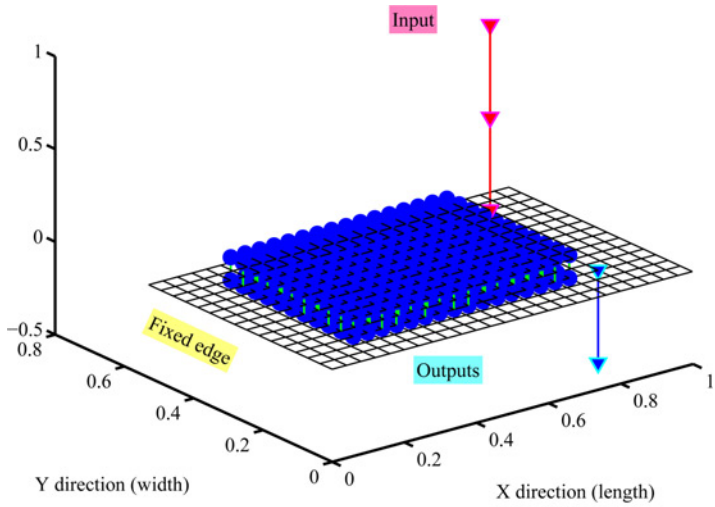

Notes: The material and geometric properties are: $L_x = 998$ mm, $L_y = 530$ mm, $t_h = 3$ mm, $\rho = 7{,}860$ kg/m^3, $E = 2.0 \times 10^5$ MPa, $\mu_r = 0.3$, $W = 12.47$ kg

Figure 4.
Finite element model of a steel cantilever plate with a damping patch

and O'Kelly, 1965; Adhikari, 2001a). Suppose the plate is excited by a unit harmonic force and the frequency response is measured at one of the nodes. If the standard four-noded thin plate bending element model is assumed, it results in 12 degrees of freedom per element. As already mentioned in section 2, the calculation of the frequency response for this kind of systems can be very expensive. Even for a relatively small case, say 25 × 15 elements, solving the linear system (2) for each frequency level can be very resource-consuming. Consider three frequency ranges, namely 0-1.0 kHz as the low-frequency range, 1.0-2.5 kHz as the medium-frequency range, and 2.5-4.0 kHz as the high-frequency range. Note that these frequency boundaries are selected on the basis of the qualitative nature of the response and devised purely for the presentation of the results.

An exploration of the applicability of emulation for six dynamical systems was carried out. Keeping the aspect ratio of the plate, an increasing number of elements (up to 50 × 30 elements and 4,650 degrees of freedom) were considered. Assuming the same boundaries for the low-, medium-, and high-frequency ranges and taking a resolution of 1 Hz, a simulator of the FRF was coded in Matlab™. For each frequency range, a training set whose size was chosen to be 5 per cent the size of the corresponding level (50 design points for low, 75 design points for medium, 75 design points for high) was selected. The corresponding training runs were obtained by solving the linear system (2) at each of the design points. Using a machine with MS Windows Vista 64 bit, 2.66 GHz Quadcore Intel Xeon Processor, and 16.0 GB RAM, an emulator of the FRF was run for the six models in each frequency range and the time employed was registered. Following Oakley and O'Hagan (2004), $\mathbf{h}(\cdot) = 1$ was assumed due to the absence of prior knowledge of the mean. This choice is not as restrictive as it might seem. Authors such as Keane and Nair (2005) note that, for a sufficiently flexible correlation structure, $\mathbf{h}(\cdot) = 1$ is often found to be suitable for modeling highly complex input-output relationships. The smoothness parameters were obtained with the method outlined in section 3. The comparison of the time taken by the simulator

and the emulator is shown in Table I. The time taken purely by the emulator, that is, disregarding the time employed in obtaining the training runs is shown in parenthesis. Note how it remains approximately constant despite the increase in resolution.

To illustrate the performance of emulation in the system with 50 × 30 elements, the predictive mean of the emulator and the corresponding probability bounds across the frequency range are shown in Figures 5-7. Note that this numerical model is aimed at representing the experimental example studied in the next section.

5. Experimental example: frequency response of a cantilever plate

5.1 Experimental setup

Suppose that the cost of obtaining measurements for a given experiment is such that they can only be generated for a very limited number of points. Also, suppose there is no suitable model to simulate the frequency response function, due perhaps to lack of knowledge about the physics of the system. In that case, the available data can be regarded as a training set upon which the emulation algorithm can be applied. In this section, an emulator is used to substitute the runs necessary to approximate experimental output (Adhikari *et al.*, 2009; Adhikari and Sarkar, 2009), whereby a cantilever plate was excited by a harmonic force and the frequency response was measured at different locations. A rectangular steel plate with the same physical and geometrical properties specified before was used, except that it had no damping patch attached. The plate was clamped along a short edge using a clamping device. The clamping device was attached to the top of a heavy concrete block and the whole assembly was placed on a steel table. Special care was taken to ensure its stability and to minimize vibration transmission. Six accelerometers were used as the response sensors. Their locations were selected such that they covered a broad area of the plate. Small holes were drilled into the plate and the accelerometers were attached by bolts through the holes. The test rig is shown in Figure 8.

5.2 Experimental methodology

Experimental modal analysis (Ewins, 2000; Maia and Silva, 1997; Silva and Maia, 1998) was used in the experiment. The three main components of the implemented experimental technique were:

(1) the excitation of the structure;

(2) the sensing of the response; and

(3) the data acquisition and processing.

Resolution		Time (s) Low frequency		Medium frequency		High frequency	
No. elements	DOF	Simulator	Emulator	Simulator	Emulator	Simulator	Emulator
25 × 15	1,200	794.28	40.47 (0.91)	1,169.72	62.87 (4.74)	1,201.85	65.71 (7.37)
30 × 18	1,710	2,098.56	106.06 (0.98)	3,149.57	160.64 (4.87)	3,107.51	162.80 (7.57)
35 × 21	2,310	4,830.03	244.50 (0.96)	7,202.22	366.02 (4.88)	7,207.08	365.68 (7.21)
40 × 24	3,000	10,040.81	499.31 (0.97)	15,025.99	749.04 (4.84)	14,934.11	759.22 (7.55)
45 × 27	3,780	19,253.25	992.63 (0.94)	29,091.82	1,429.92 (4.86)	29,787.58	1,495.28 (7.62)
50 × 30	4,650	35,273.89	1,763.70 (0.97)	53,107.12	2,437.01 (4.83)	56,063.20	2,781.38 (7.49)

Notes: The numbers in parenthesis are the time employed purely by the emulator, without taking into account the computation of the training runs

Table I. Computation time in seconds of the simulator against the emulator, for the three frequency ranges and different resolutions

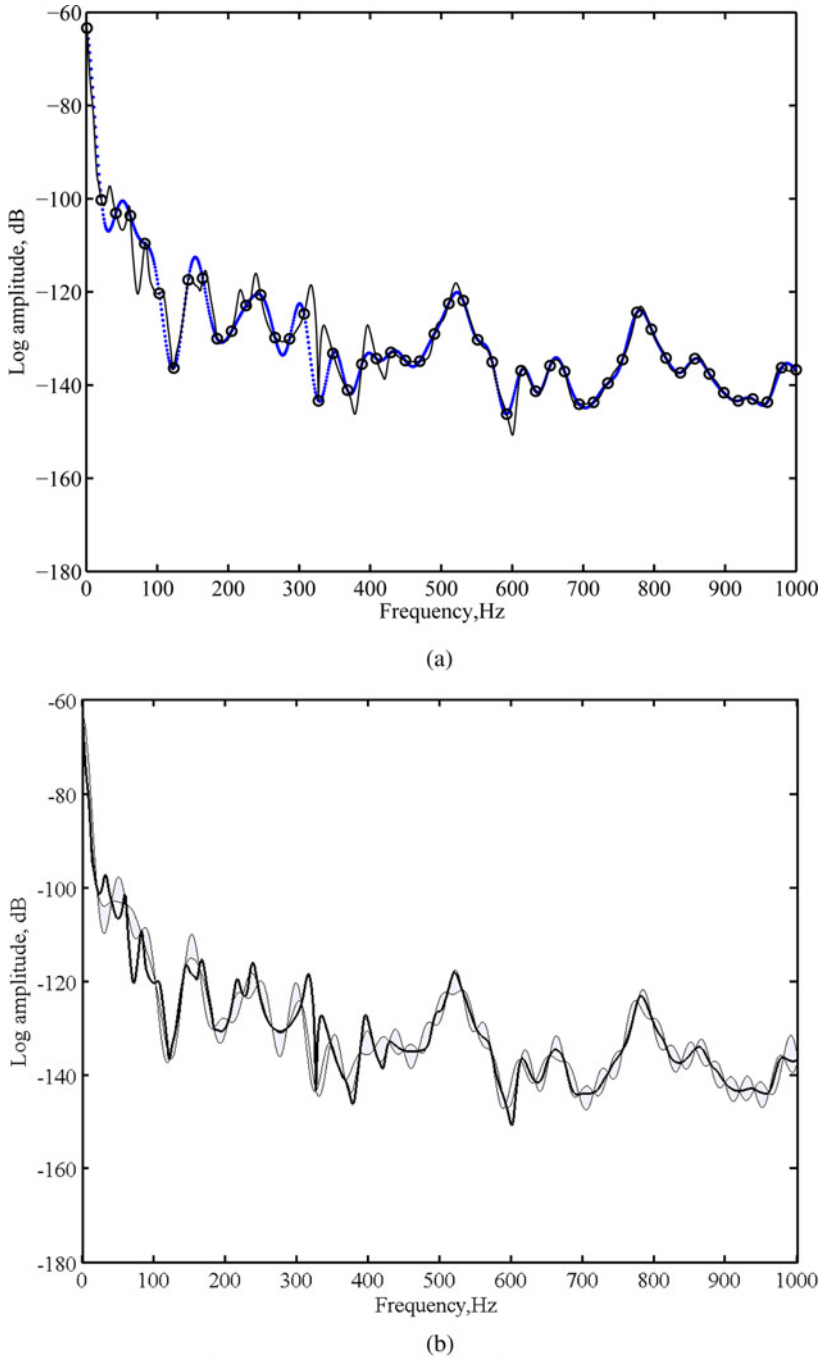

Figure 5.
Emulation of the response in the low-frequency range with 50 design points

Notes: (a) Mean of the emulator and (b) probability bounds for the mean (shaded areas); (-): simulator's output, (o): training runs, (···): emulator's predictive mean

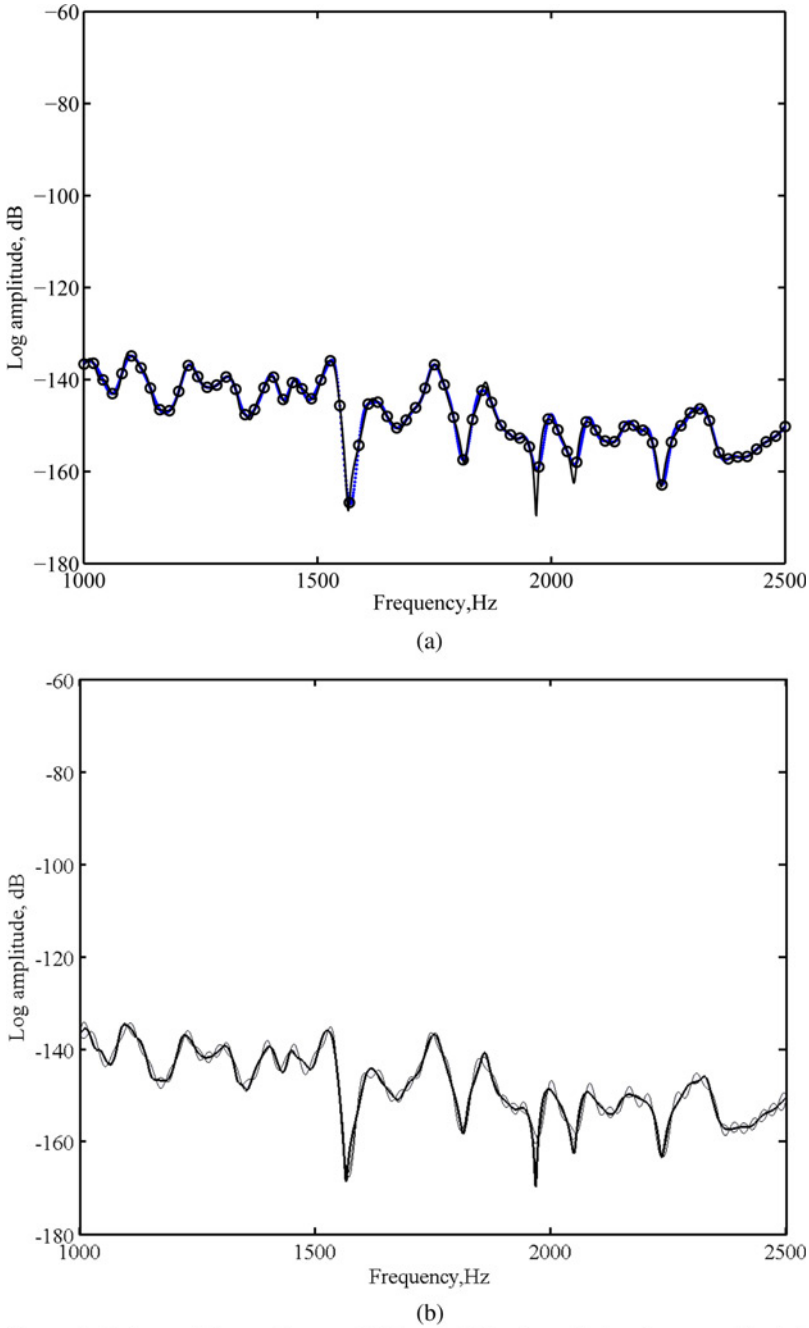

Notes: (a) Mean of the emulator and (b) probability bounds for the mean (shaded areas); (-): simulator's output, (o): training runs, (···): emulator's predictive mean

Figure 6.
Emulation of the response in the medium-frequency range with 75 design points

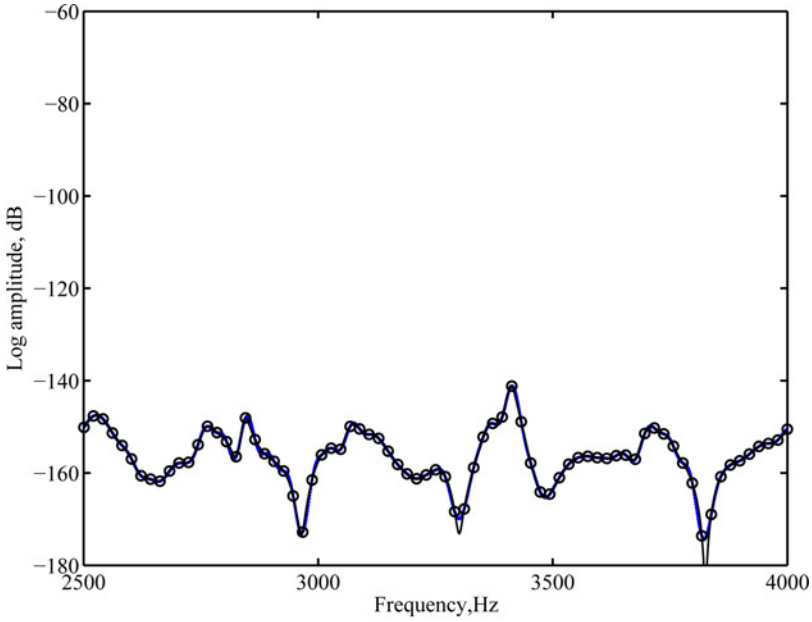

(a)

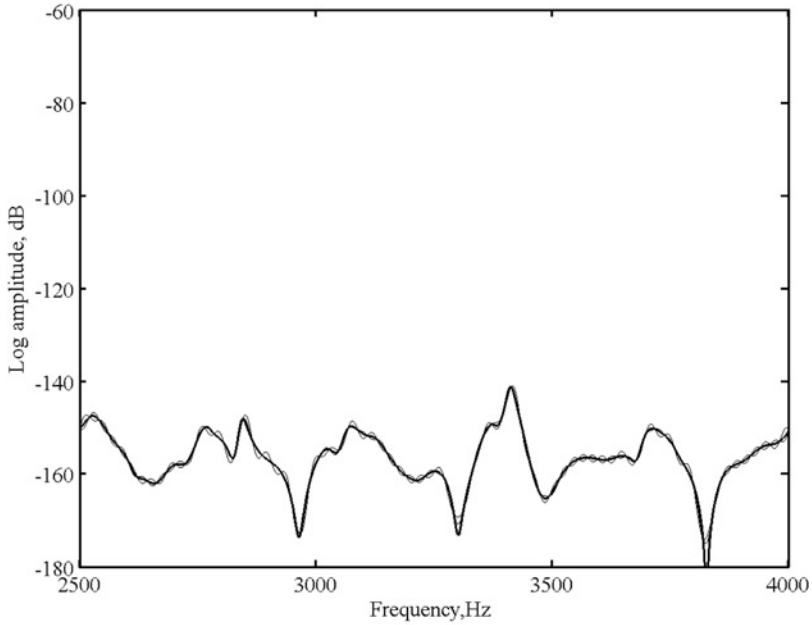

(b)

Notes: (a) Mean of the emulator and (b) probability bounds for the mean (shaded areas); (-): simulator's output, (o): training runs, (···): emulator's predictive mean

Figure 7.
Emulation of the response in the high-frequency range with 75 design points

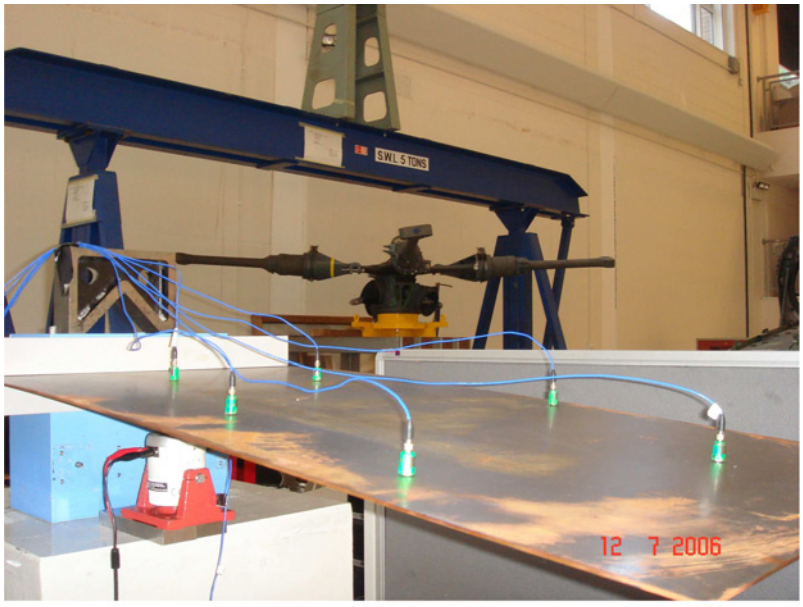

Notes: A steel cantilever plate was excited by a harmonic force and the frequency response was measured. Six accelerometers were used as the response sensors. Their locations were selected to cover a broad area of the plate

Figure 8.
Experimental setup

A shaker was used to act as an impulse hammer. The shaker generated impulses at a pulse interval of 20 s and a pulse width of 0.01 s. It was placed so that it impacted at a particular node of the plate. It was driven by a signal from a Simulink™ and dSpace™ system via a power amplifier. A hard steel tip is used for the hammer to increase the frequency range of excitation. The steel tip used in the experiment only gave clean data up to approximately 4,500 Hz. Therefore, 4,000 Hz was used as the upper limit of the frequency in the measured frequency response functions. The data logged beyond 4,000 Hz were ignored. The data obtained are available on the world wide web for research purposes at: http://engweb.swan.ac.uk/~adhikaris/uq/

5.3 Emulation of experimental data

Emulation was performed to approximate the response of one of the nodes to vibration in the three frequency ranges, where 50, 75, and 75 design points were, respectively employed. Analogously to the emulation of simulated data in section 4, $\mathbf{h}(\cdot) = 1$ was assumed due to the absence of prior knowledge of the mean. The smoothness parameters were obtained with the method mentioned in section 3. The results are shown in Figures 9-11.

Note that the number of design points for each frequency range was chosen arbitrarily. However, if it were truly expensive to carry out the experiment, the number of design points would depend on the cost of generating data. Moreover, the experimental data for every frequency level would not be available for comparison with the emulator's predictive mean. This brings up the problem of measuring if the simulator is a suitable representation of the emulator. This problem is addressed in section 7.

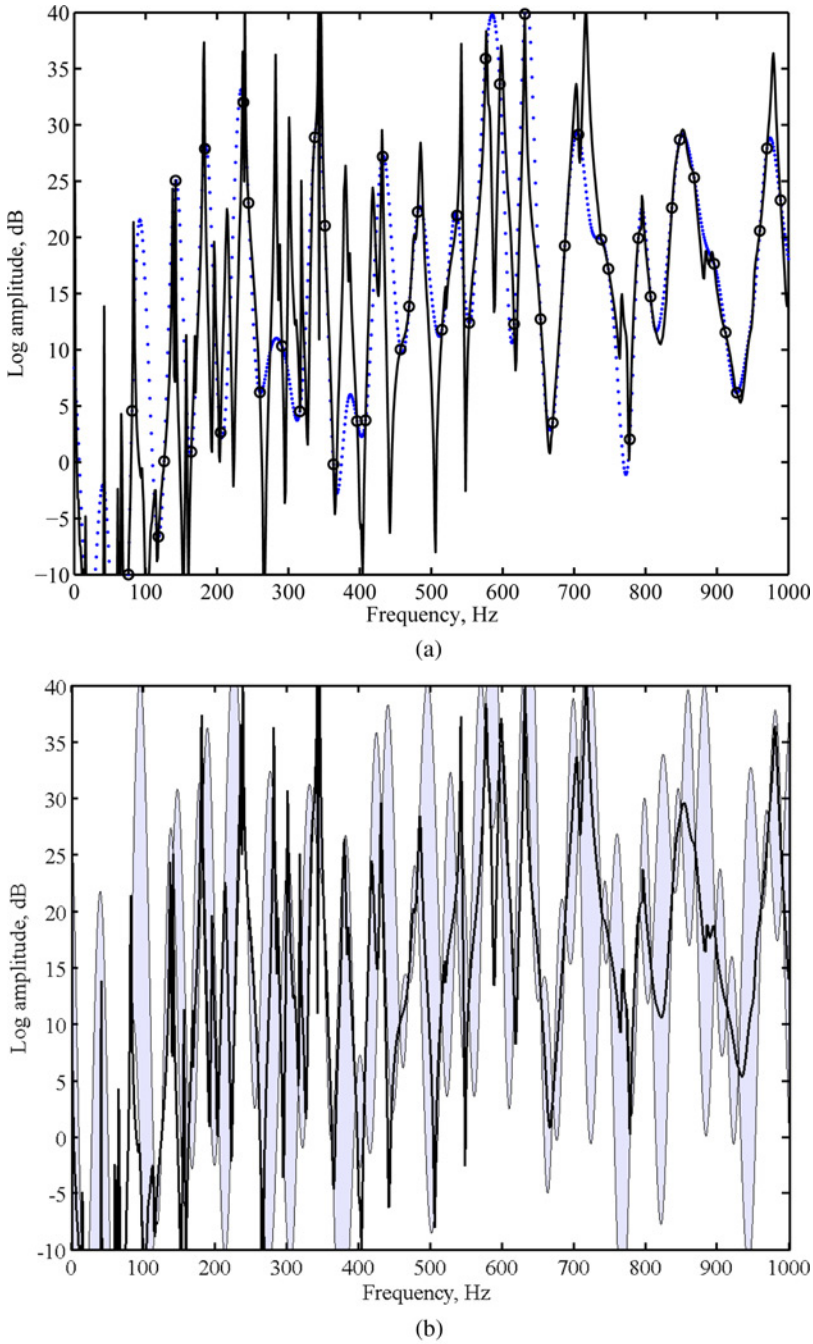

Figure 9.
Emulation of the response in the low-frequency range with 50 design points obtained from the experiment

Notes: (a) Mean of the emulator and (b) probability bounds for the mean (shaded areas); (-): experimental results, (o): training runs, (···): emulator's predictive mean

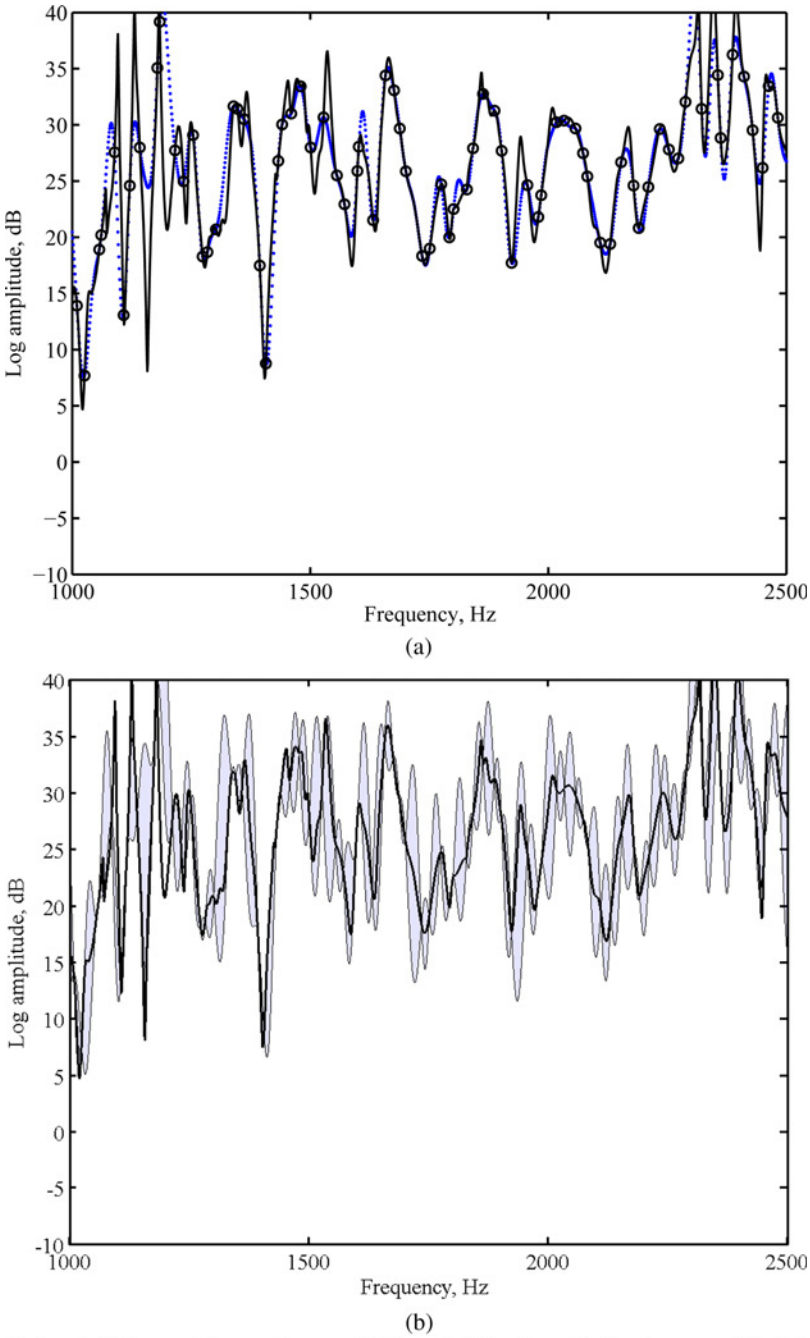

Notes: (a) Mean of the emulator and (b) probability bounds for the mean (shaded areas); (-): experimental results, (o): training runs, (···): emulator's predictive mean

Figure 10.
Emulation of the response in the medium-frequency range with 75 design points obtained from the experiment

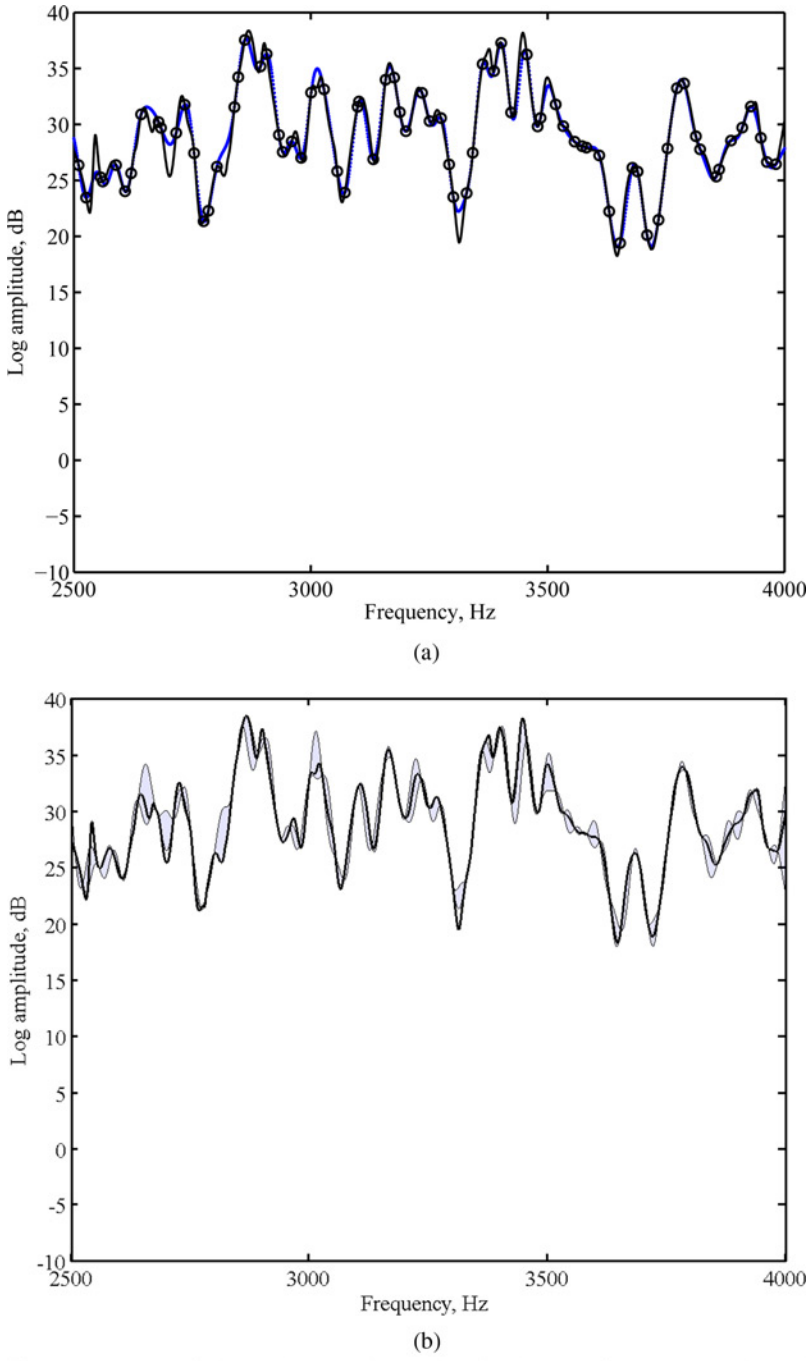

Figure 11.
Emulation of the response in the high-frequency range with 75 design points obtained from the experiment

Notes: (a) Mean of the emulator and (b) probability bounds for the mean (shaded areas); (-): experimental results, (o): training runs, (···): emulator's predictive mean

6. Discussion of the method and the results

Based on the above results, it can be argued that the use of emulators in the context of structural dynamics can help to approach the following questions:

- *Efficiency* – Can the output of a structural dynamics simulator be approximated using only a few trial runs?
- *Computational cost* – Can the number of floating point operations and the CPU time employed by an expensive simulator be dramatically reduced but still produce a satisfactory output?
- *Interpolation of experimental data* – Can expensive experimental data be confidently interpolated to cope with the lack of a mathematical or computational model?

Regarding the first question, an emulator for the simple spring-mass system in section 3 illustrates how the predictive mean can be a plausible approximation to the corresponding FRF. Related to the second question, the dynamic response of systems with up to 4,650 degrees of freedom was emulated in section 4. Note that when the complete model was run, the linear system (2) had to be solved 4,000 times. Adopting the emulator approach, it had to be solved only 200 times, equivalent to the number of training runs necessary to approximate the output across the frequency range. The saving in CPU time was considerable and it was observed that the computational burden was mainly due to the calculation of the training runs, not to the emulation itself. From the figures presented, the approximation looks particularly appealing for the medium- and high-frequency ranges where the frequency response function is smoother compared to that in the low-frequency region. This is encouraging since these are the computationally demanding ranges of vibration where numerical models of real-life systems can have several millions of degrees of freedom. With regards to the third question, an FRF obtained via experimental modal analysis was emulated in section 5. Real test data were used as the set of training runs necessary to construct an emulator and the experimental output was compared with the corresponding approximation.

As mentioned before, an emulator is a statistical approximation to the simulator. For both the simulated and the experimental examples presented here, the predictive mean and the corresponding uncertainty bounds were provided. This is one of the main differences between emulation and traditional interpolation techniques: emulation provides a probability distribution and thus a method of quantifying the uncertainty that arises from being able to evaluate the simulator very few times. In the examples presented, the emulator's output seemed to represent the simulator's output fairly well. Note, however, that visual inspection is not enough to rigourously determine the quality of the agreement between the simulator's output and the emulator's predictive mean. Despite the computation time for some of the simulators employed took tenths of hours, it was still possible to obtain their output on the entire frequency range. For more expensive systems, the comparison of the simulator's output against the emulator's predictive mean would be, by definition, only possible in a very reduced number of points. Visual inspection would be unable to detect whether the emulator misrepresents the simulator's output, in which case, all inferences made using the emulator would be spurious. Moreover, in case of having more than two inputs, graphical comparison is not possible. It is therefore important to have a suitable means of assessing the adequacy of Gaussian process emulators.

7. Emulator validation

Although the Gaussian process is a flexible class of distributions to represent prior beliefs about a computer model, an emulator might poorly represent the simulator due to a wrong choice of the mean and covariance structures or a wrong choice of the training set that might induce an inappropriate estimation of parameters. To cope with these disadvantages, Bastos and O'Hagan (2008) proposed several methods for the validation of the emulators, some of which were applied to the results presented above.

Let $\Omega^* = \{\omega_1^*, \ldots, \omega_v^*\}$ be a set of validation points in the frequency domain, different from the already chosen design points, but similarly chosen using a criterion such as Latin hypercube sampling. The corresponding validation data are $\mathbf{y}^* = [\eta(\omega_1^*), \ldots, \eta(\omega_v^*)]^T$. One possible diagnostic of $\mathbf{y}^*$ is to calculate the standardized prediction errors of the simulator's output and the predictive mean of the emulator given the training data. That is, for $j = 1, \ldots, v$:

$$\delta_j^{se}(\mathbf{y}^*) = \frac{\mathbf{y}_j^* - m^{**}(\eta(\omega_j^*))}{\widehat{\sigma}\sqrt{C^{**}(\eta(\omega_j^*), \eta(\omega_j^*))}} \tag{14}$$

Each one of these standardized prediction errors has a Student's t-distribution, conditional on original vector of observations $\mathbf{y}$ (and on the smoothness parameters). Note that the size of the training data can be large enough such that $\delta_j^{se}(\mathbf{y}^*)$ approximates a standard normal distribution. Therefore, $|\delta_j^{se}(\mathbf{y}^*)| > 2$ for a high j would hint inadequacy of the Gaussian process emulator in a neighborhood of ω_j^*.

The emulation of experimental data in section 5 was validated using this measure. The validation set was chosen to have 50 validation points. Figure 12(a) plots the predictive mean of the emulator against the standardized errors in the medium-frequency range. This graph can help to identify problems in the specification of the predictive mean, a situation that would be evident if, for example, most of the points lied in the positive area or vice versa. Additionally, Figure 12(b) is the plot of the validation points against the standardized errors. This graph can be used to identify areas of the input domain for which the emulator misrepresents the simulator. In this case, a Gaussian process emulator appeared to be a sensible choice to represent the simulator, confirming what had been suggested by Figure 10. Similarly satisfactory results were obtained for each of the frequency ranges. For the sake of brevity, only the ones corresponding to the medium-frequency range are displayed.

A disadvantage of using the individual standardized errors is that correlation between the elements of the validation data set is not taken into account. Another possibility is to employ the Mahalanobis distance of $\mathbf{y}^*$, defined as:

$$\delta_{MD}(\mathbf{y}^*) = \{\mathbf{y}^* - \mathbf{m}^{**}[\eta(\Omega^*)]\}^T \mathbf{V}[\eta(\Omega^*)]^{-1} \{\mathbf{y}^* - \mathbf{m}^{**}[\eta(\Omega^*)]\} \tag{15}$$

where

$$\mathbf{m}^{**}[\eta(\Omega^*)] = [m^{**}(\eta(\omega_1^*)), \ldots, m^{**}(\eta(\omega_v^*))]^T \tag{16}$$

is the vector of individual predictive means and $\mathbf{V}[\eta(\Omega^*)]^{-1}$ is the inverse of the emulator's conditional covariance matrix expressed by equation (25) in the Appendix. Note that it can be decomposed such that $\mathbf{V} = \mathbf{G}\mathbf{G}^T$. That way, the vector of validation errors is:

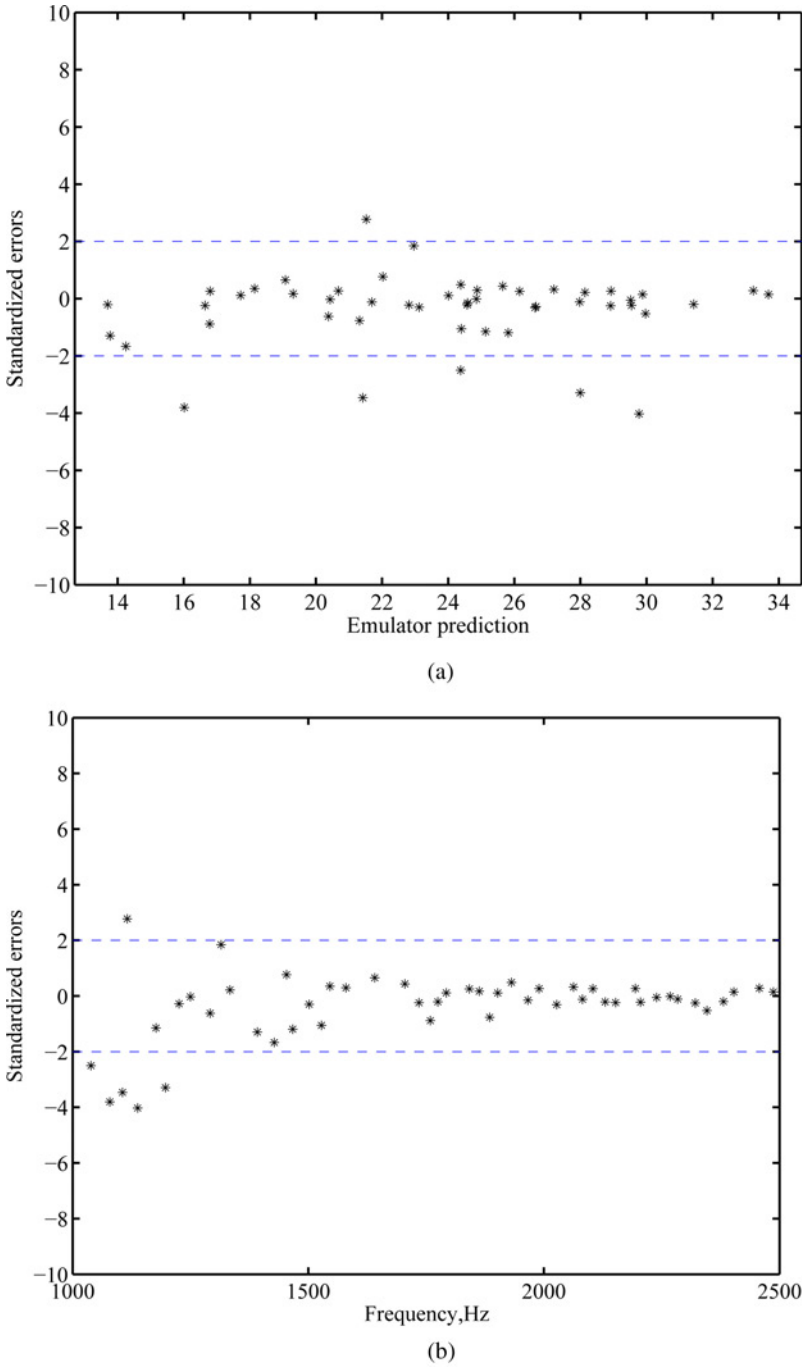

Notes: (a) Predictive means vs standardized errors and (b) validation points vs standardized errors; medium-frequency range

Figure 12.
Individual standardized errors diagnostics

$$\boldsymbol{\delta}_{\mathbf{G}}(\mathbf{y}^*) = \mathbf{G}^{-1}\{\mathbf{y}^* - \mathbf{m}^{**}[\eta(\Omega^*)]\} \tag{17}$$

which implies that the Mahalanobis distance can be decomposed as:

$$\delta_{MD}(\mathbf{y}^*) = \boldsymbol{\delta}_{\mathbf{G}}(\mathbf{y}^*)^T \boldsymbol{\delta}_{\mathbf{G}}(\mathbf{y}^*). \tag{18}$$

One available strategy to obtain **G** is the pivoting Cholesky decomposition. It has the property of permuting the individual validation errors in equation (17), such that they are decreasingly ordered with respect to their variance. Figure 13 shows the individual validation errors, plotted against the index of the ordered validation data. An implementation of the pivoting Cholesky decomposition is provided by Higham at http://www.ma.man.ac.uk/~higham/mctoolbox/. Again, the adequacy of the emulator was sought to be confirmed by the validation errors being uniformly spread around zero.

8. Conclusions and future developments

Based on encouraging results from various scientific disciplines, this paper proposes the adoption of Gaussian process emulators as an efficient predictive computational approach in structural dynamics. The capabilities of this computational tool were tested in both simulated and experimental contexts. The FRFs of several dynamical systems were emulated and the results were contrasted with the output of the original simulators. An FRF obtained via experimental methods was also emulated. Real data were used as the set of training runs and the experimental output was compared with the corresponding approximation. The results were particularly appealing in the medium- and high-frequency ranges. Since the validation of Gaussian process emulators as appropriate surrogate models cannot be carried out only by visual

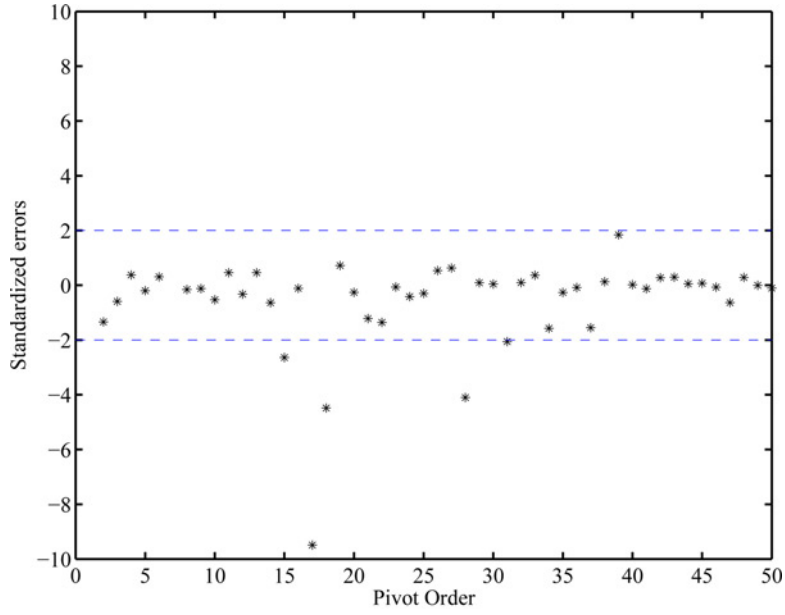

Note: Medium-frequency range

Figure 13.
Pivoting Cholesky decomposition diagnostics

inspection, some diagnostics of adequacy were implemented, and the agreement between a simulator's and an emulator's output was verified.

There are two potential advantages of using the proposed emulator-based approach for structural dynamics. The first is that the computational cost is practically independent of the damping model. This is due to the fact that the cost of solving the linear system (2) at the training frequency points does not depend on whether the underlying damping model is viscous, viscoelastic, or any other frequency-dependent damping model. The second advantage arises from the fact that once the training frequency points are selected, the linear system (2) can be solved at those points in parallel. On top of it, each solution can be efficiently parallelized, for example using the conventional domain decomposition methods (Smith *et al.*, 2004; Quarteroni and Valli, 1999; Mathew, 2008), since the dynamic stiffness matrix is highly banded in nature. Further studies are however, needed to exploit the potential parallel computation capabilities of the proposed approach.

References

Adhikari, S. (1999), "Modal analysis of linear asymmetric non-conservative systems", *ASCE Journal of Engineering Mechanics*, Vol. 125 No. 12, pp. 1372-79.

Adhikari, S. (2001a), "Classical normal modes in non-viscously damped linear systems", *AIAA Journal*, Vol. 39 No. 5, pp. 978-80.

Adhikari, S. (2001b), "Eigenrelations for non-viscously damped systems", *AIAA Journal*, Vol. 39 No. 8, pp. 1624-30.

Adhikari, S. (2002), "Dynamics of non-viscously damped linear systems", *ASCE Journal of Engineering Mechanics*, Vol. 128 No. 3, pp. 328-39.

Adhikari, S. (2004), "Optimal complex modes and an index of damping non-proportionality", *Mechanical System and Signal Processing*, Vol. 18 No. 1, pp. 1-27.

Adhikari, S. and Sarkar, A. (2009), "Uncertainty in structural dynamics: experimental validation of wishart random matrix model", *Journal of Sound and Vibration*, Vol. 323 Nos 3-5, pp. 802-25.

Adhikari, S. and Wagner, N. (2003), "Analysis of asymmetric non-viscously damped linear dynamic systems", *Transactions of ASME, Journal of Applied Mechanics*, Vol. 70 No. 6, pp. 885-93.

Adhikari, S. and Wagner, N. (2004), "Direct time-domain approach for exponentially damped systems", *Computer and Structures*, Vol. 82 Nos 29/30, pp. 2453-61.

Adhikari, S. and Woodhouse, J. (2003), "Quantification of non-viscous damping in discrete linear systems", *Journal of Sound and Vibration*, Vol. 260 No. 3, pp. 499-518.

Adhikari, S.M.I., Friswell, K.L. and Sarkar, A. (2009), "Experimental uncertainty quantification in structural dynamics", *Probabilistic Engineering Mechanics*, Vol. 24 No. 4, pp. 473-92.

Bastos, L. and O'Hagan, A. (2008), "Diagnostics for gaussian process emulators", Technical Report No. 574/08, Department of Probability and Statistics, University of Sheffield, Sheffield.

Bates, R., Kennet, R., Steinberg, D. and Wynn, H. (2006), "Achieving robust design from computer simulations", *Quality Technology & Quantitative Management*, Vol. 3 No. 2, pp. 161-77.

Bathe, K.-J. (1995), *Finite Element Procedures*, Prentice-Hall, Englewood Cliffs, NJ.

Caughey, T.K. and O'Kelly, M.E.J. (1965), "Classical normal modes in damped linear dynamic systems", *Transactions of ASME, Journal of Applied Mechanics*, Vol. 32, pp. 583-8.

Challenor, P., Hankin, R. and Marsh, R. (2006), "Achieving robust design from computer simulations", *Avoiding Dangerous Climate Change*, Cambridge University Press, Cambridge.

Cook, R.D., Malkus, D.S., Plesha, M.E. and Witt, R.J. (2001), *Concepts and Applications of Finite Element Analysis*, 4th ed., John Wiley & Sons, New York, NY.

Craig, K.J., Stander, N., Dooge, D.A. and Varadappa, S. (2005), "Automotive crashworthiness design using response surface-based variable screening and optimization", *Engineering Computations*, Vol. 22 No. 1, pp. 38-61.

Ewins, D. J. (2000), *Modal Testing: Theory and Practice*, 2nd ed., Research Studies Press, Baldock.

Fan, H., Lampinen, J. and Levy, Y. (2006), "An easy-to-implement differential evolution approach for multi-objective optimizations", *Engineering Computations*, Vol. 23 No. 2, pp. 124-38.

Goldstein, M. (2007), "Uncertainty analysis for complex physical models", *30th Research Student's Conference in Probability and Statistics in Public Resource, 27-29 March, Durham*.

Haylock, R. and O'Hagan, A. (1996), *Bayesian Statistics 5*, Oxford University Press, Oxford.

Hughes, T.J.R. (2000), *The Finite Element Method: Linear Static and Dynamic Finite Element Analysis*, Dover Publications, New York, NY.

Kennedy, M.C. and O'Hagan, A. (2001), "Bayesian calibration of computer models", *Journal of the Royal Statistical Society Series B-Statistical Methodology*, Vol. 63 No. 3, pp. 425-50.

Kennedy, M.C., Anderson, C.W., Conti, S. and O'Hagan, A. (2006), "Case studies in gaussian process modelling of computer codes", *Reliability Engineering & System Safety*, Vol. 91 Nos 10/11, pp. 1301-09.

Kleijnen, J.P.C. (2009), "Kriging metamodeling in simulation: a review", *European Journal of Operational Research*, Vol. 192 No. 3, pp. 707-16.

Krzanowski, W. (2000), *Principles of Multivariate Analysis*, Oxford University Press, Oxford.

McFarland, J., Mahadevan, S., Romero, V. and Swiler, L. (2008), "Calibration and uncertainty analysis for computer simulations with multivariate output", *49th AIAA/ASME/ASCE/AHS/ASC Structures, Structural Dynamics & Materials Conference, AIAA, Schaumburg, IL*.

McKay, M., Conover, W. and Beckman, R. (1979), "A comparison of three methods for selecting values of input variables in the analysis of output from a computer code", *Technometrics*, Vol. 21 No. 2, pp. 239-45.

Maia, N.M.M. and Silva, J.M.M. (Eds) (1997), *Theoretical and Experimental Modal Analysis*, Engineering Dynamics Series, Research Studies Press, Taunton.

Maia, N. M. M., Silva, J. M. M., and Ribeiro, A. M. R. (1998), "On a general model for damping", *Journal of Sound and Vibration*, Vol. 218 No. 5, pp. 749-67.

Mathew, T. (2008), *Domain Decomposition Methods for the Numerical Solution of Partial Differential Equations*, Springer Verlag, Berlin and Heidelberg, GmbH & Co, Berlin.

Newland, D.E. (1989), *Mechanical Vibration Analysis and Computation*, Longman, Harlow and John Wiley, New York, NY.

Oakley, J. (2004), "Estimating percentiles of computer code outputs", *Applied Statistics* Vol. 53, pp. 83-93.

Oakley, J.E. and O'Hagan, A. (2004), "Probabilistic sensitivity analysis of complex models: A Bayesian approach", *Journal of the Royal Statistical Society B*, Vol. 66 No. 3, pp. 751-69.

O'Hagan, A. (1994), "Bayesian inference", *Kendall's Advanced Theory of Statistics*, Vol. 2B, Arnold, London.

O'Hagan, A. (2006), "Bayesian analysis of computer code outputs: a tutorial", *Reliability Engineering & System Safety*, Vol. 91 Nos 10/11, pp. 1290-300.

Pérez, V.M., Renaud, J.E. and Watson, L.E. (2008), "Reduced sampling for construction of quadratic response surface approximations using adaptive experimental design", *Engineering Computations*, Vol. 25 No. 8, pp. 764-82.

Petyt, M. (1998), *Introduction to Finite Element Vibration Analysis*, Cambridge University Press, Cambridge.

Quarteroni, A. and Valli, A. (1999), *Domain Decomposition Methods for Partial Differential Equations*, Oxford University Press, Oxford.

Rayleigh, L. (1877), *Theory of Sound* (two volumes), 1945 re-issue, 2nd ed., Dover Publications, New York, NY.

Rougier, J. (2007), "Probabilistic inference for future climate using an ensemble of climate model evaluations", *Climatic Change*, Vol. 81 No. 3, pp. 247-64.

Rougier, J., Sexton, D., Murphy, M. and Stainforth, D. (2007), "Emulating the sensitivity of the HadSM3 climate model using ensembles from different but related experiments", Technical Report No. 07/04, MUCM, University of Sheffield, Sheffield.

Sacks, J., Welch, W., Mitchell, T. and Wynn, H. (1989), "Design and analysis of computer experiments", *Statistical Science*, Vol. 4 No. 4, pp. 409-35.

Satner, T., Williams, B. and Notz, W. (2003), *The Design and Analysis of Computer Experiments*, Springer Series in Statistics, London.

Silva, J.M.M. and Maia, N.M.M. (Eds) (1998), *Modal Analysis and Testing: Proceedings of the NATO Advanced Study Institute*, NATO Science Series: E: Applied Science, Sesimbra.

Simpson, T.W., Mauery, T.M., Korte, J.J. and Mistree, F. (2001), "Kriging meta-models for global approximation in simulation-based multidisciplinary design optimization", *AIAA Journal*, Vol. 39 No. 12, pp. 2233-41.

Smith, B., Bjorstad, P. and Gropp, W. (2004), *Domain Decomposition: Parallel Multilevel Methods for Elliptic Partial Differential Equations*, Cambridge University Press, Cambridge.

Sultan, I.A. (2007), "A surrogate model for interference prevention in the limaçon-to-limaçon machines", *Engineering Computations*, Vol. 24 No. 5, pp. 437-49.

Thomke, S., Holzner, M. and Gholami, T. (1999), "The crash in the machine", *Scientific American*, Vol. 280 No. 3, pp. 92-7.

Torvik, P.J. and Bagley, R.L. (1987), "Fractional derivatives in the description of damping: materials and phenomena", in *The Role of Damping in Vibration and Noise Control*, ASME DE-5, pp. 125-35.

Wagner, N. and Adhikari, S. (2003), "Symmetric state-space formulation for a class of non-viscously damped systems", *AIAA Journal*, Vol. 41 No. 5, pp. 951-6.

Woodhouse, J. (1998), "Linear damping models for structural vibration", *Journal of Sound and Vibration*, Vol. 215 No. 3, pp. 547-69.

Zhao, M., Huang, Z. and Chen, L. (2008), "Multidisciplinary design optimization of tool head for heavy duty CNC vertical turning mill", *Engineering Computations*, Vol. 25 No. 7, pp. 657-76.

Zienkiewicz, O.C. and Taylor, R.L. (1991), *The Finite Element Method*, 4th ed., McGraw-Hill, London.

Further reading

Biot, M.A. (1958), "Linear thermodynamics and the mechanics of solids", *Proceedings of the Third US National Congress on Applied Mechanics*, ASME, New York, NY, pp. 1-18.

Haylock, R. (1996), "Bayesian inference about outputs of computationally expensive algorithms with uncertainty on the inputs", PhD thesis, University of Nottingham, Nottingham.

Keane, A. and Nair, P. (2005), *Computational Approaches for Aerospace Design*, John Wiley & Sons, Chichester.

Appendix

The following is an outline of the prior-to-posterior analysis discussed in subsection 3.2. Full details can be found in O'Hagan (1994), Haylock and O'Hagan (1996), and Oakley (2004).

Suppose that the simulator's output $\eta(\omega)$ at an untried input ω is to be estimated. Let $\mathbf{y} = [\eta(\omega_1), \ldots, \eta(\omega_n)]^T$ be a vector of observations. Define $\mathbf{H} = [\mathbf{h}(\omega_1), \ldots, \mathbf{h}(\omega_n)]^T$ and $\mathbf{A} \in \mathbb{R}^{n \times n}$ with $\mathbf{A}_{\ell j} = C(\omega_\ell, \omega_j)\ \forall \ell, j \in \{1, \ldots, n\}$; where $\mathbf{h}$ follows from equation (9) and $C(\cdot, \cdot)$ is the correlation function defined by equation (11). Thus, the prior distribution (12) can be recast as:

$$\mathbf{y}|\beta, \sigma^2 \sim \mathcal{N}(\mathbf{H}\beta, \sigma^2\mathbf{A}) \tag{19}$$

In order to incorporate the objective information $\mathbf{y}$ and obtain the distribution of $\eta(\cdot)|\mathbf{y}$, use the following result, given in Krzanowski (2000).

Theorem. Let $\mathbf{z} \in \mathbb{R}^d$ be a random vector such that $\mathbf{z} \sim \mathcal{N}(\mu, \Sigma)$. Partition $\mathbf{z}$ as $(\mathbf{z}_1, \mathbf{z}_2)^T$, where $\mathbf{z}_1 \in \mathbb{R}^p$ and $\mathbf{z}_2 \in \mathbb{R}^{d-p}$. Consequently, partition $\mu = (\mu_1, \mu_2)^T$ and $\Sigma = \begin{pmatrix} \Sigma_{11} & \Sigma_{12} \\ \Sigma_{21} & \Sigma_{22} \end{pmatrix}$, so that $\mathbf{E}[\mathbf{z}_j] = \mu_j$ and $Cov(\mathbf{z}_j, \mathbf{z}_k) = \Sigma_{jk}$. Then, $\mathbf{z}_1|\mathbf{z}_2 \sim \mathcal{N}(\widetilde{\mu}, \widetilde{\Sigma})$, where $\widetilde{\mu} = \mu_1 + \Sigma_{12}\Sigma_{22}^{-1}(\mathbf{z}_2 - \mu_2)$ and $\widetilde{\Sigma} = \Sigma_{11} - \Sigma_{12}\Sigma_{22}^{-1}\Sigma_{21}$.

From this, it follows that

$$\eta(\cdot)|\mathbf{y}, \beta, \sigma^2 \sim \mathcal{N}(m^*(\cdot), \sigma^2 C^*(\cdot, \cdot)) \tag{20}$$

where, if the vector $\mathbf{t}(\omega) = [C(\omega, \omega_1), \ldots, C(\omega, \omega_n)]^T$ is defined, then:

$$m^*(\omega) = \mathbf{h}(\omega)^T\beta + \mathbf{t}(\omega)\mathbf{A}^{-1}(\mathbf{y} - \mathbf{H}\beta) \tag{21}$$

$$C^*(\omega, \omega') = C(\omega, \omega') - \mathbf{t}(\omega)^T A^{-1}\mathbf{t}(\omega') \tag{22}$$

Haylock and O'Hagan (1996) note that knowing the value of β or σ^2 beforehand is usually unrealistic. They show that, carrying out the suitable integration, the conditioning on β can be removed to obtain the posterior distribution:

$$\eta(\cdot)|\mathbf{y}, \sigma^2 \sim \mathcal{N}(m^{**}(\cdot), \sigma^2 C^{**}(\cdot, \cdot)) \tag{23}$$

where

$$m^{**}(\omega) = \mathbf{h}(\omega)^T\widehat{\beta} + \mathbf{t}(\omega)\mathbf{A}^{-1}(\mathbf{y} - \mathbf{H}\widehat{\beta}) \tag{24}$$

$$\begin{aligned} C^{**}(\omega, \omega') = C^*(\omega, \omega') &+ (\mathbf{h}(\omega)^T - \mathbf{t}(\omega)^T\mathbf{A}^{-1}\mathbf{H})(\mathbf{H}^T\mathbf{A}^{-1}\mathbf{H})^{-1} \\ &\times (\mathbf{h}(\omega')^T - \mathbf{t}(\omega')^T\mathbf{A}^{-1}\mathbf{H})^T \end{aligned} \tag{25}$$

$$\widehat{\beta} = (\mathbf{H}^T\mathbf{A}^{-1}\mathbf{H})^{-1}\mathbf{H}^T\mathbf{A}^{-1}\mathbf{y} \tag{26}$$

To estimate σ in (23), it can be shown (O'hagan, 1994) that

$$\widehat{\sigma}^2 = \frac{\mathbf{y}^T(\mathbf{A}^{-1} - \mathbf{A}^{-1}\mathbf{H}(\mathbf{H}^T\mathbf{A}^{-1}\mathbf{H})\mathbf{H}^T\mathbf{A}^{-1})\mathbf{y}}{n-q-2} \tag{27}$$

where q is the rank of $\mathbf{H}$. Note that the posterior distribution (23) is also a Gaussian process distribution. From equation (24) it can be seen that $m^{**}(\cdot)$ does not include any terms involving $\eta(\cdot)$. Thus, it provides a fast approximation of $\eta(\omega)$ for any ω. The conditioning on σ^2 can also be eliminated, such that:

$$\frac{\eta(\omega) - m^*(\omega)}{\widehat{\sigma}\sqrt{\frac{(n-q-2)C^*(\omega)}{n-q}}} \sim t_{n-q} \tag{28}$$

which is a Student's t-distribution with $n-q$ degrees of freedom (not to be confused with the degrees of freedom in a finite element method context).

About the authors

F.A. DiazDelaO is a postgraduate student at Swansea University, where he was awarded a studentship from the Engineering and Physical Sciences Research Council (EPSRC) and a scholarship by the Mexican National Council for Science and Technology (CONACYT). He holds a BSc in Applied Mathematics from the Autonomous Technological Institute of Mexico (ITAM) and an MSc in Statistics and Operational Research from the University of Essex, UK. The PhD project he is currently working on is titled "Coupled models: expert judgment, emulators and model uncertainty". This project is funded by the EPSRC's ideas factory grant to encourage multidisciplinary research. F.A. DiazDelaO is the corresponding author and can be contacted at: diazdelao@yahoo.com.mx

S. Adhikari is currently an EPSRC Advanced Research Fellow (4 September-9 August) and a Professor of Aerospace Engineering in Swansea University (from April 2007). He was the winner of the prestigious Philip Leverhulme Prize (2007) in Engineering (given to an outstanding scholar under the age of 35). He received his PhD in 2001 (as a Jawaharlal Nehru Memorial Trust scholar at the Trinity College) from the University of Cambridge. He was a lecturer at the Bristol University (3 January-7 March) and a Junior Research Fellow in fitzwilliam College, Cambridge (1 September-3 January). He was a visiting Professor at the Carleton University (Canada, 2006) and a visiting scientist at the Los Alamos National Laboratory (USA, 2006). From May to December 2008 he is an official visitor to the Cambridge University Engineering Department and a visiting Fellow of Fitzwilliam College, Cambridge. S. Adhikari's research areas are multidisciplinary in nature and include structural dynamics and vibration control, model identification and validation, reliability-based optimal design, earthquake engineering, groundwater flow problems, probabilistic methods in structural mechanics, nanomechanics and wind energy quantification. He has published 62 journal papers and 68 conference papers in these areas.